American Journal of Civil Engineering and Architecture, 2022, Vol. 10, No. 3, 106-115
Available online at http://pubs.sciepub.com/ajcea/10/3/1
Published by Science and Education Publishing
DOI:10.12691/ajcea-10-3-1

Blast Loading Resistance of Metro Tunnel in Shale Rock: A Coupled-Eulerian-Lagrangian (CEL) Approach

Mohd Shoeb[1], Mohd. Evan[1], Mohammad Anas[1], Mohammad Arif Kamal[2,*]

[1]Department of Geology, Faculty of Science, Aligarh Muslim University, Aligarh, India
[2]Architecture Section, Faculty of Engg. & Technology, Aligarh Muslim University, Aligarh, India
*Corresponding author: architectarif@gmail.com

Received June 10, 2022; Revised July 14, 2022; Accepted July 24, 2022

Abstract The internal blast loading condition in a tunnel constructed in three-layered shale rock has been incorporated using a coupled-eulerian-lagrangian (CEL) approach in this paper. In this research, the three weathered stages of shale were studied, namely minimally, medium, and highly weathered shale in three layers. As we got closer to the earth's surface from the deep beneath, the weathering of the shale rock accelerates. The overburden depth has been changed to integrate several parametric scenarios in an elastoplastic finite element model with dimensions of 60m x 60m x 60m. The presence of 100kg of trinitrotoluene (TNT) as an explosive is expected A 100kg of trinitrotoluene (TNT) explosive is assumed to be suspended in the air at the middle of the tunnel entrance at an equal distance from all sides. To recreate genuine in-situ conditions, the TNT sphere and air inside the rock tunnel were modeled using the CEL approach. Mohr-Coulomb, Concrete Damage Plasticity, and Johnson-Cook constitutive material models were used to mimic the elastoplastic behavior of various materials, including rock, concrete, and steel bars. To make a reinforced concrete liner, a cage of steel bars has been inserted in the concrete liner by interaction constraints. The tunnel was first buried in the upper layer of shale, with a 5m overburden depth. The tunnel's position has also been altered for overburden depths of 15m, 25m, and 35m. Overburden depth and crown displacement are inversely proportional, according to the results obtained in the form of acceleration, velocity, and displacement for rock. Furthermore, the reinforced concrete liner used in this simulation study exhibits no damage in terms of compression, although a small tensile failure is visible in all scenarios.

Keywords: *blast loading, weathering, tunnel, shale, Abaqus, Coupled-Eulerian-Lagrangian (CEL)*

Cite This Article: Mohd Shoeb, Mohd Evan, Mohammad Anas and Mohammad Arif Kamal, "Blast Loading Resistance of Metro Tunnel in Shale Rock: A Coupled-Eulerian-Lagrangian (CEL) Approach." *American Journal of Civil Engineering and Architecture*, vol. 10, no. 3 (2022): 106-115. doi: 10.12691/ajcea-10-3-1.

1. Introduction

Tunnel construction has become an inseparable component of modern metro cities as transportation and the design of speedier modes for products and services inside and between cities have given rise to tunnel development on a bigger scale [1]. As a result, experienced personnel are required to develop and plan these smart, long-term structures. Tunnels, in addition to being a source of transportation, have become an integral aspect of a country's strategic defense system [2]. As a result, the stability of tunnels under massive loads, both accidental and purposeful, has been a great concern. Several research on the stability of various types of structures subjected to extreme loading conditions, such as blast load, have been done [3-10].

The first collection of studies to understand the damage in rock tunnels due to seismic shaking was presented by [11]. Later on, the influence switched away from earthquakes and toward rock blasting. Accidental events, such as terror strikes may involve the use of heavy explosives, on the other hand. Terrorist events such as the 1993 World Trade Center bombings, as well as the 1994 bombings of London and Buenos Aires financial hubs, have prompted researchers to investigate the blast-resistance of tunnels using various simulation tools. As a result of the blast loading induced by missile attacks, structures should be designed with blast resistance in consideration to reduce the damage caused by an impact missile [12].

The freshness of the rock or how much it has weathered determines its strength. Rock weathering can be both mechanical and chemical. Mechanical weathering is the fracture and abrasion of rock into smaller pieces; it aids chemical weathering by causing the breakdown of rock into smaller pieces, which increases the total surface area vulnerable to chemical weathering. Weathering weakens rock's resistance to blasting and makes it more susceptible to it. Bowen's reaction series best explains its progression. The ascending order of stability means resistance to weathering: Olivine, Orthopyroxene, Clinopyroxene, Amphibole, Biotite, K- Feldspar, Muscovite, and Quartz.

Since brick masonry is a basic structural component of every conventional building, its blast resistance has been

examined using the finite element approach for blast-resistant structural design. Reference [13] used the commercial program Abaqus / Explicit to conduct a finite element study of a reinforced wall. It has been discovered that the diameter of steel reinforcement bars and concrete grade indicate that concrete grade and wall thickness have a substantial relationship with deformation and damage produced by blast loading. Reference [14] investigated the effects of blast load on fracture propagation and concrete. A constitutive material model was proposed to anticipate the progression of crack damage and propagation. Later, [15] investigated the effect of strain rate, both high and low, to provide more in-depth data for predicting concrete response under dynamic loading. Reference [16] conducted rigorous parametric research for an underground tube surrounded by rock and soil. They used the Monte Carlo method and the Abaqus finite element software. When the tunnel is subjected to blasting load, failure is observed to be a function of Young's modulus, tunnel lining thickness, and blast loading. They stated that in the case of blast loading studies of tunnels, both probabilistic and deterministic approaches to analysis should be explored. Furthermore, the explosive weight and charge chamber density have a considerable impact on the density of explosive charge loading and the strength of the stress wave [17].

Researchers have conducted several studies to better understand the response of tunnels to various types of loading events, including blast loading [18-29]. The impact of weathering, on the other hand, has received little attention in the literature. Furthermore, the stratified rock profile has scarcely been taken into account while simulating the real field condition of a tunnel that has been built.

2. Nonlinear Elastoplastic Continuum Modelling

The present study incorporates three different weathered shale rocks, i.e., slightly weathered, medium weathered and highly weathered, where slightly weathered shale is at the bottommost layer having 20m of thickness. Similarly, a middle layer of 20m thickness of the finite element model consists of medium weathered shale rock and the top layer is made up of highly weathered shale having 20m of thickness. Initially, the tunnel has been considered in the top layer with 5m of overburden depth for the first case of analysis. Later, the overburden depth of the tunnel has been increased by 10m intervals. Therefore, in two cases the tunnel has a half-top portion in the upper layer of rock and a half-bottom portion in the lower layer of rock. The finite element model having 60m x 60m x 60m of size has been modeled in the Abaqus/Explicit module to create a continuum model with finite element definition. The various causes have been considered in this study by considering overburden depths as 5m, 15m, 25m and 35m. The TNT has 100kg of mass in the form of a sphere, which is hanging in the air at equal distance from all sides. The tunnel has been supported by a 10m diameter tunnel having 0.35m of thickness having 12mm diameter steel bars @ 120mm spacing along the length of the tunnel as twin-circular rings (spacing = 250mm) to act as hoop reinforcement. Moreover, longitudinal reinforcement bars having a 10mm diameter have been provided along the circular direction with 850mm of circular spacing (Limited 2015). This reinforcement cage which is made up of Fe415 grade steel is surrounded by a concrete liner of M30 grade. Figure 1 represents the detailed geometry of the finite element tunnel model.

The present finite element method of analysis has an elastoplastic nonlinear behavior of different weathered shale rocks that have been considered through the Mohr-Coulomb failure criterion. The properties of slightly, medium and higher stages of weathered shale are presented in Table 1. These properties have been taken from [30] and substituted in Abaqus for each grade of shale. The three layers of shale stratified as, less weathered shale at a deeper level and more weathered occurring at shallow depth from the surface. The thickness of each layer of weathered shale has been kept constant at 20m each.

Table 1. Mohr-Coulomb Material Model Properties Of Different Weathered Grades Of Shale [30]

Sydney Shale	Slightly Weathered	Medium Weathered	Highly Weathered
Mass Density (kg/m^3)	2400	2400	2400
Young's Modulus (MPa)	4500	2000	1000
Poisson's Ratio	0.25	0.25	0.30
Friction Angle (^{o})	50	50	40
Cohesion (kPa)	500	300	200

The tunnel in the different layer has been supported by an M30 grade concrete liner that is reinforced with steel bars. The nonlinear elastoplastic properties of tunnel liner made up of concrete have been simulated through Concrete Damage Plasticity (CDP) criterion. Table 2 & Table 3 and Figure 2 & Figure 3 represent the input parameters of CDP model for M30 grade concrete [31].

Table 2. Elastoplastic properties of concrete having M30 grade [30]

Parameter	Value
Mass Density (kg/m^3)	2500
Young's Modulus (GPa)	26.6
Poisson's Ratio	0.2
Dilation Angle (^{o})	31
Eccentricity	0.1
fb0/fc0	1.16
k	0.67
Viscosity Parameter	0

Table 3. Tension Failure Parameters Used In The Present Study For M30 Grade Concrete [31]

Tensile Behavior	
Stress (MPa)	Strain
2.00	0
0.02	0.000943396
Tensile Damage	
Damage	Strain
0.00	0
0.99	0.000943396

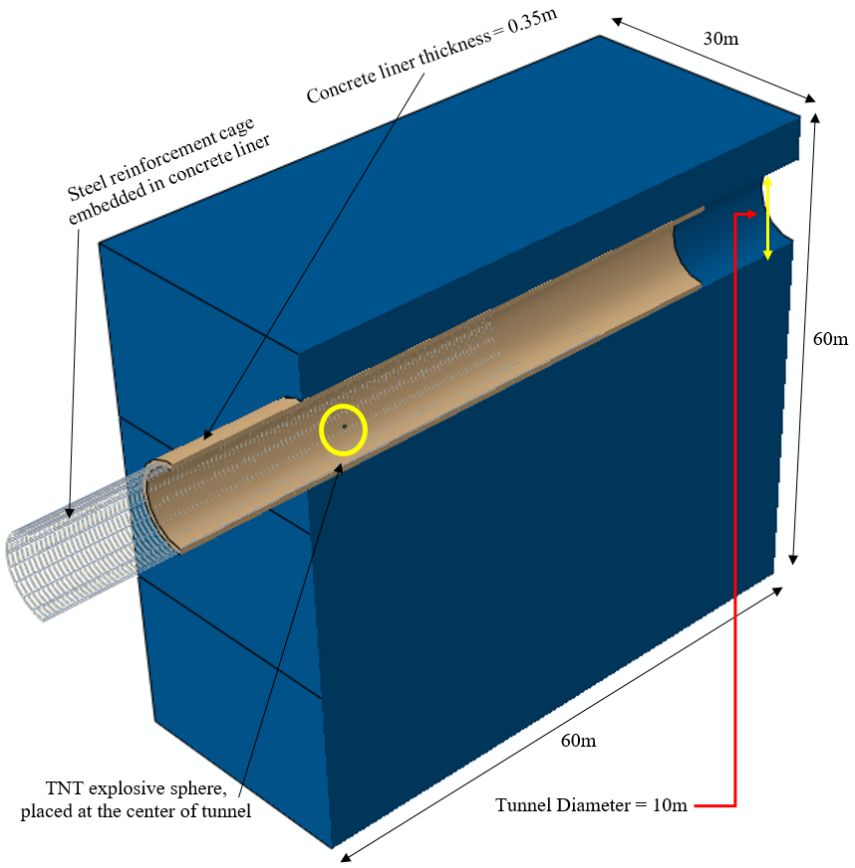

Figure 1. Detailed geometry of present numerical model used in the present

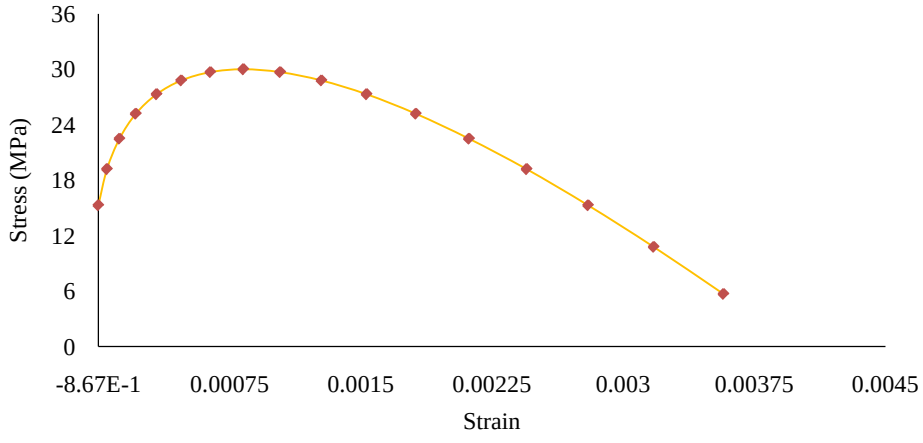

Figure 2. Variation of stress with change in strain for M30 grade of concrete [30]

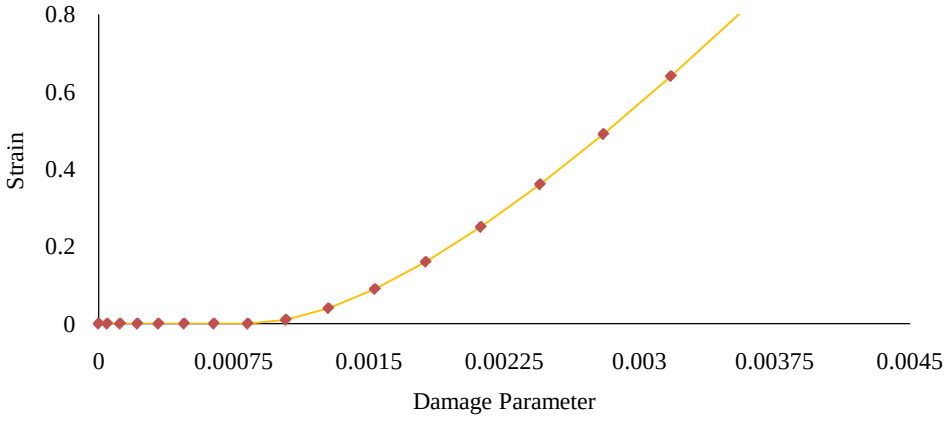

Figure 3. Variation of damage with strain in case of M30 concrete grade [30]

The steel reinforcing bars were implanted in the concrete liner of the tunnel utilizing the Abaqus/Explicit interaction module's embedment constraint. To simulate the nonlinear elastoplastic behavior of steel bars, the Johnson-Cook material model was used. The input parameters of the Johnson-Cook steel model are shown in Figure 4 and Table 4 (IS: 456(2000).

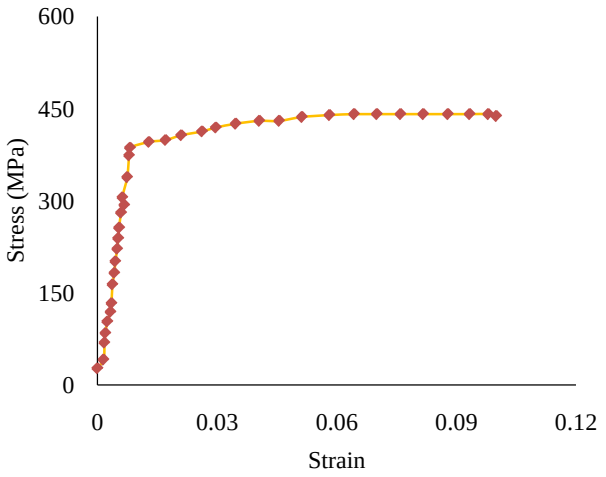

Figure 4. Variation of stress with change in strain for Fe415 steel grade (IS 456, 2000)

Table 4. Parameters Used For Steel Bars Used As Reinforcement [31]

Parameter	Value
Mass Density (kg/m^3)	7800
Young's Modulus (GPa)	210
Poisson's Ratio	0.3
A (MPa)	375
B (MPa)	600
n	0.07
C	0.09
Strain Rate (s^{-1})	50

The properties of Trinitrotoluene (TNT) used in the presented simulation are presented in Table 5. Jones-Wilkins-Lee (JWL) constitutive material model has been adopted to incorporate the nonlinear elastoplastic behavior of TNT and the Equation-of-State (EOS) definition of JWL has been considered.

Table 5. JWL-EOS Parameters Adopted In The Present Study For TNT Explosive (Larcher And Casadei, 2010)

Parameter	**Value**
Mass Density (kg/m^3)	1630
Detonation Wave Speed (m/s)	6930
A (GPa)	373.8
B (GPa)	3.747
ω	0.35
R_1	4.15
R_2	0.9
Detonation Energy Density (kJ/kg)	3680

The field circumstances in this study were constructed and recreated by giving boundary conditions such as the rock's base has fixed supports in all directions, and the vertical sides have roller supports that allow nodes to move vertically. Because the depth of rock at the base is unclear, the base has been limited in all directions. Due to the known finite width of the rock block, the sides also have roller support. A commonly used interaction, general contact, has been included in the Abaqus/Explicit interaction module to capture the hardness of each section of the model. The default setting for the interaction is in the tangential and normal directions. Self-friction has been postulated between the rock, concrete liner, and reinforcing cage steel bars.

Based on the mesh convergence analysis shown in Figure 5, the rock and concrete liner element type has been chosen as C3D8R, with each element having a size of 0.8. Because this element type contains eight nodes and a brick-like shape, it is known as an 8-noded brick element. The element type's other parameters are left at their default values. Because the steel bars are wires, they mesh with the B31 element type, which is a 2-noded beam type element. The steel bar cage was implanted inside the concrete liner of the tunnel utilizing embedment constraint in the interaction module after all of the outer and inner steel bars were assembled in the assembly module. Other settings are left at their default to ensure that the steel bars of the reinforcement cage and the concrete liner are properly bonded to work as reinforced concrete material.

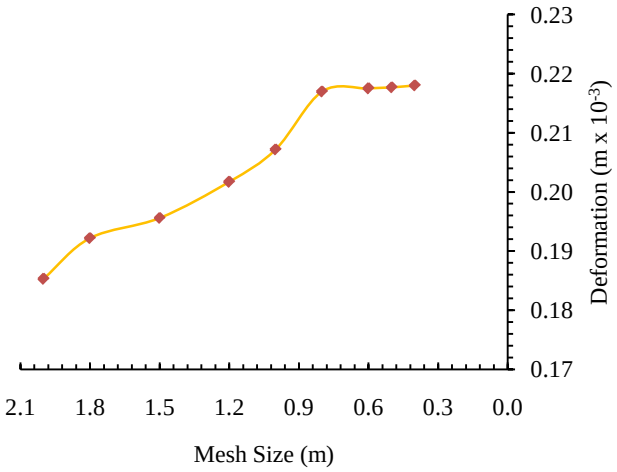

Figure 5. Mesh convergence study for element size determination

To model TNT explosives to induce internal blast loading in the current study, JWL-EOS was used to build Coupled-Eulerian-Lagrangian (CEL) modeling. The main benefit of employing this technology is that the mistake that occurs in these types of simulations may be mitigated. In general, ambient air has not been considered in earlier research; nevertheless, it has been considered in the current case in tunnel opening and around the explosive sphere of TNT. The EC3D8R element type was used to mesh the CEL component of the model, where 'E' stands for Eulerian. Eulerian-Volume-Friction (EVF) is a discrete field that has been assigned to the models in the predefined field. Based on prior investigations, EVF = 1.0 has been attributed to TNT and EVF = 0.8 has been assigned to the air inside the tube [32-36]. To mimic the internal blast loading, a 100 kg TNT explosive has been assumed and put in the tunnel's middle part, at an equal distance from the tunnel's interior surface.

3. CEL Model Validation

The validation of blast loading using the CEL modeling technique was accomplished by comparing the results of [37], which were provided through a numerical and experimental investigation, with the numerical model built using the current methodology. The geometry, characteristics, and loading conditions are all preserved the same as they were in the original design [37]. In Figure 6, the results of the current modeling technique and [37] are compared. The findings show that the current modeling technique has been proven and may be applied to future simulations.

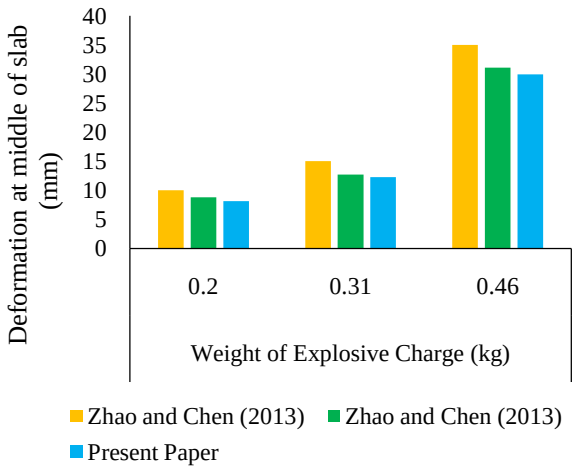

Figure 6. Validation of CEL modeling [37]

4. Results and Discussion

The influence of stratification and weathering on the internal blast resistance of a shale rock tunnel was studied using nonlinear elastoplastic continuum finite element modeling. The overburden depth has been changed so that in two cases, the tunnel remains completely in a single layer, while in two other situations, half of the tunnel is in one layer and half in the other. The current section of the paper presents the results obtained using the coupled-eulerian-lagrangian elastoplastic continuous finite element technique.

The behavior of rock under internal blast loading due to TNT explosives with various tunnel positions has been compared in Figure 7. In each example, the displacement contours of varied overburden depths illustrated in Figure 7 indicate that the explosion effect has reached the ground surface. However, as the overburden depth increases, the amount of displacement reduces, hence displacement is inversely proportional to the overburden depth. Displacement has also been seen to reduce up to 25m of overburden depth before increasing due to the overburden load of two worn shale rocks. Maximum displacement is 17.58mm, 6.34mm, 0.786mm, and 1.55mm for overburden depths of 5m, 15m, 25m, and 35m, respectively. It has been determined that a 25-meter-deep tunnel is 7 times more resistant to internal blast loading than a 15-meter-deep overburden tunnel. Similarly, a tunnel with 15 meters of overburden depth has 1.77 times the blasting resistance.

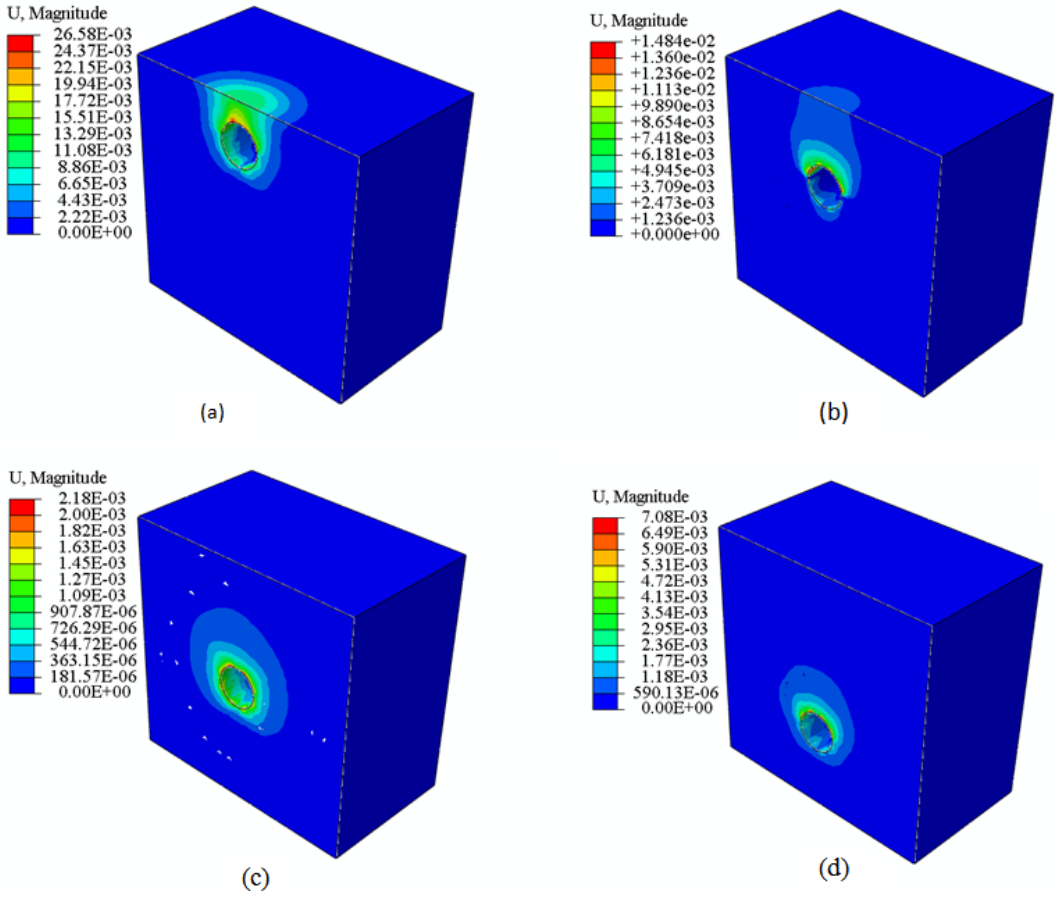

Figure 7. Contours of displacement in case of (a) 5m, (b) 15m, (c) 25m and (d) 35m of overburden depth

For varied overburden depths, the displacement profile has been presented along the ground surface in Figure 8. The displacement concentration is found to be close to the location of the blast loading event in each case. However, the amplitude of displacement at the center is greater than at other nodal sites, and it decreases as we move away from the source. The largest displacement magnitude is for a 5m overburden depth scenario, which is 10-times bigger. However, in other overburden depth situations, the difference between the amounts of displacement at the ground is much smaller. Furthermore, because the tunnel was built in weathered shale rock, blast loading caused the most damage. As a result, it has been discovered that weathering has a significant impact on the blast resistance of underground tubes.

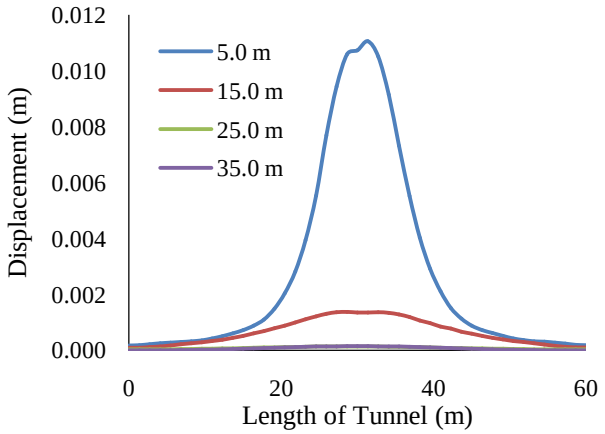

Figure 8. Displacement profile at the ground of tunnel for an event of internal blast loading for different overburden depths

The variation of displacement with time has been plotted to understand the behavior of rock tunnels during an event of blast loading and it has been plotted in Figure 9. It has been observed from the graphs of different overburden depths that shallow rock tunnels in highly weathered shale rock have suffered extreme damage from the initial time when blast wave intersects with the tunnel lining. An exponential increase in displacement has been observed throughout the analysis; however, as the overburden depth of the tunnel increases the displacement variation with time becomes more linear. It has also been concluded that shallow rock tunnels are highly susceptible to blast loading in comparison to deeper tunnels as observed in previous cases.

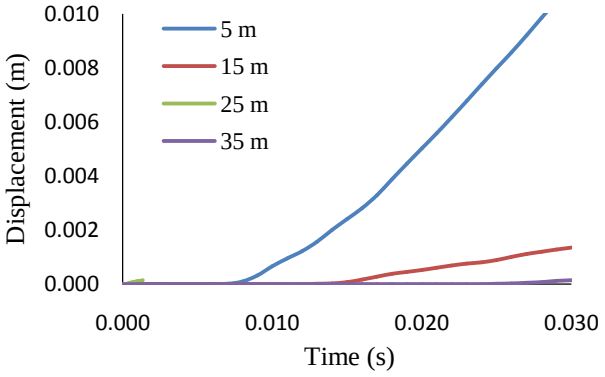

Figure 9. Variation of displacement at the ground of the tunnel with time during an event of internal blast loading for different overburden depths

Figure 10 has been plotted to compare the variation of velocity in different cases of overburden with time. The behavior of rock tunnels under blast loading follows a similar trend in all the cases, however, the magnitude of velocity is inversely proportional to the overburden depth of the tunnel, and it is directly proportional to the degree of weathering. It has been noted that the magnitude of velocity at the ground surface decreased sharply when overburden depth has been increased by 10m and resulted in 15m of overburden depth. However, there has been a lesser difference in the magnitude of velocity for 25m and 35m of overburden depth. Similarly, Figure 11 has been plotted to compare the acceleration produced by an internal blast loading due to 100kg of TNT explosive. The trend of acceleration variation with time has similarities for the different cases of overburden depth, however, the magnitude in the case of 5m overburden depth and highly weathered shale has the highest magnitude which reduces with an increase in the magnitude of overburden depth. In addition, it has been observed that if the rock has been subjected to lesser weathering, then, it has higher blast resistance.

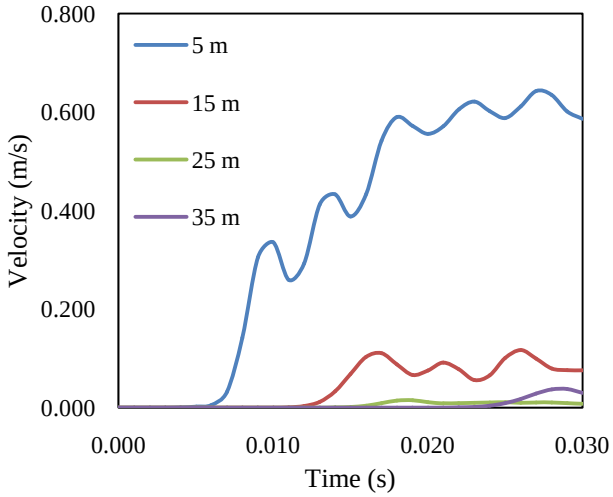

Figure 10. Variation of velocity at the ground of the tunnel with time during an event of internal blast loading for different overburden depths

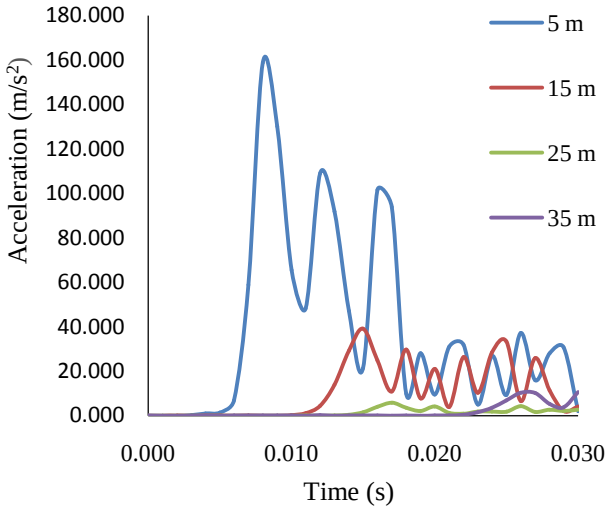

Figure 11. Variation of acceleration at the ground of tunnel with time during an event of internal blast loading for different overburden depths

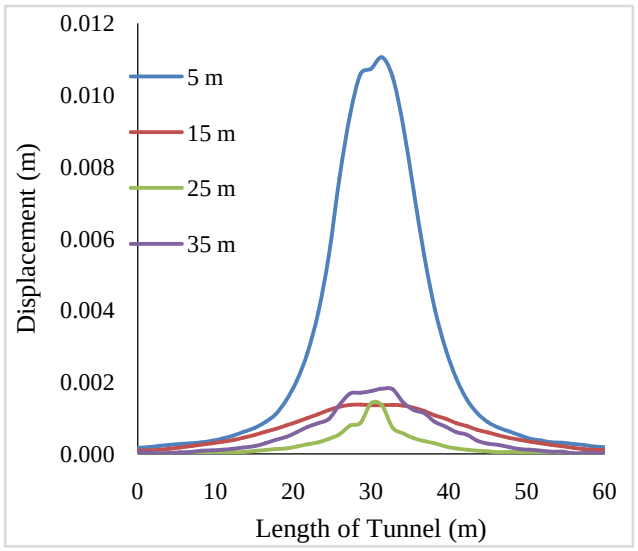

Figure 12. Displacement profile at the crown of the tunnel for an event of internal blast loading for different overburden depths

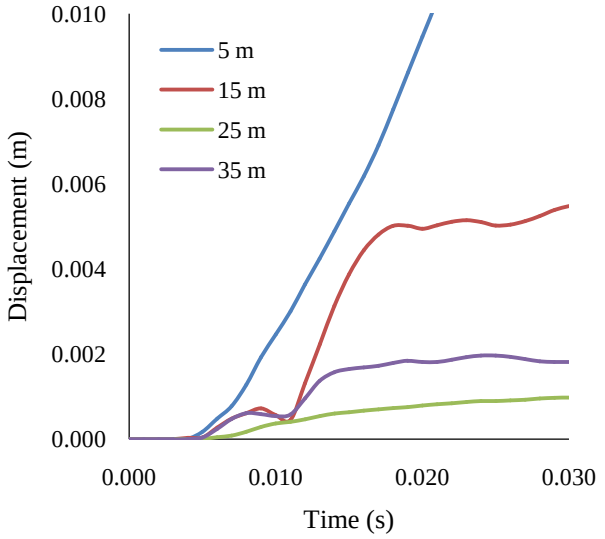

Figure 13. Variation of displacement at the crown of the tunnel with time during an event of internal blast loading for different overburden depths

The results obtained at the crown of the tunnel suggest an in-depth observation of tunnel stability in rock, therefore, Figure 12 has been plotted to compare the displacement profile obtained for different overburden depths along the crown of the tunnel when subjected to internal blast loading due to 100kg of TNT explosive. In the case of 5m of overburden depth, the displacement profile does not follow an ideal trend but shows a peak at the center of the tunnel. The most vulnerable case in the present study has been noted as 5m overburden depth as it has the highest and most extreme displacement magnitude in all the cases. However, the other cases of overburden depth such as 15m, 25m and 35m have slight uniform behavior and displacement reduces uniformly in these three cases, while a sudden decrease in the magnitude has been observed when overburden depth increases from 5m to 15m. A similar trend has been observed in Figure 13, where the variation of displacement has been plotted with time for different overburden depths. The magnitude of displacement noted for 15m, 25m and 35m are in close vicinity while 5m overburden depth has a magnitude of displacement that is several times the other cases.

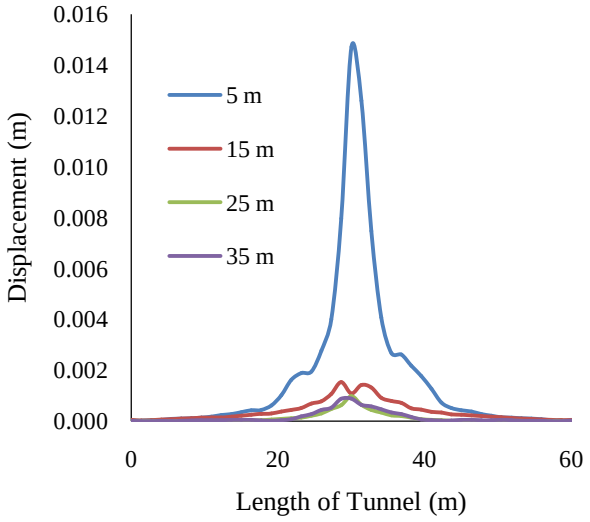

Figure 14. Displacement profile at the invert of the tunnel for an event of internal blast loading for different overburden depths

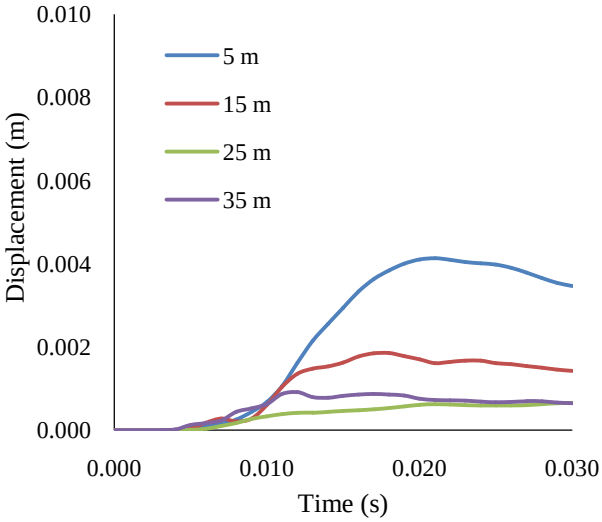

Figure 15. Variation of displacement at the invert of the tunnel with time during an event of internal blast loading for different overburden depths

Figure 14 has been plotted to compare the displacement profile in different cases of overburden depth in the stratified shale rock mass. In the case of inverting the difference between the magnitude of displacement for 5m and 15m overburden depths has been reduced in comparison to ground and crown locations. Moreover, it has been observed that the entire length of the tunnel has been under the effect of blast loading along the invert and maximum magnitude has been concentrated at the center of the tunnel where the internal blast has occurred. Also, the displacement in the case of 35m of overburden depth has been constant throughout the length of the tunnel along the invert. Figure 15 has been plotted to compare the displacement variation with time at the center node of the tunnel at the inverted location. The displacement behavior has been similar in all the cases of overburden depth as observed in previous Figures. However, in previous cases, only 5m of overburden depth has significant displacement magnitude, but at an invert location, the displacement has considerable magnitude.

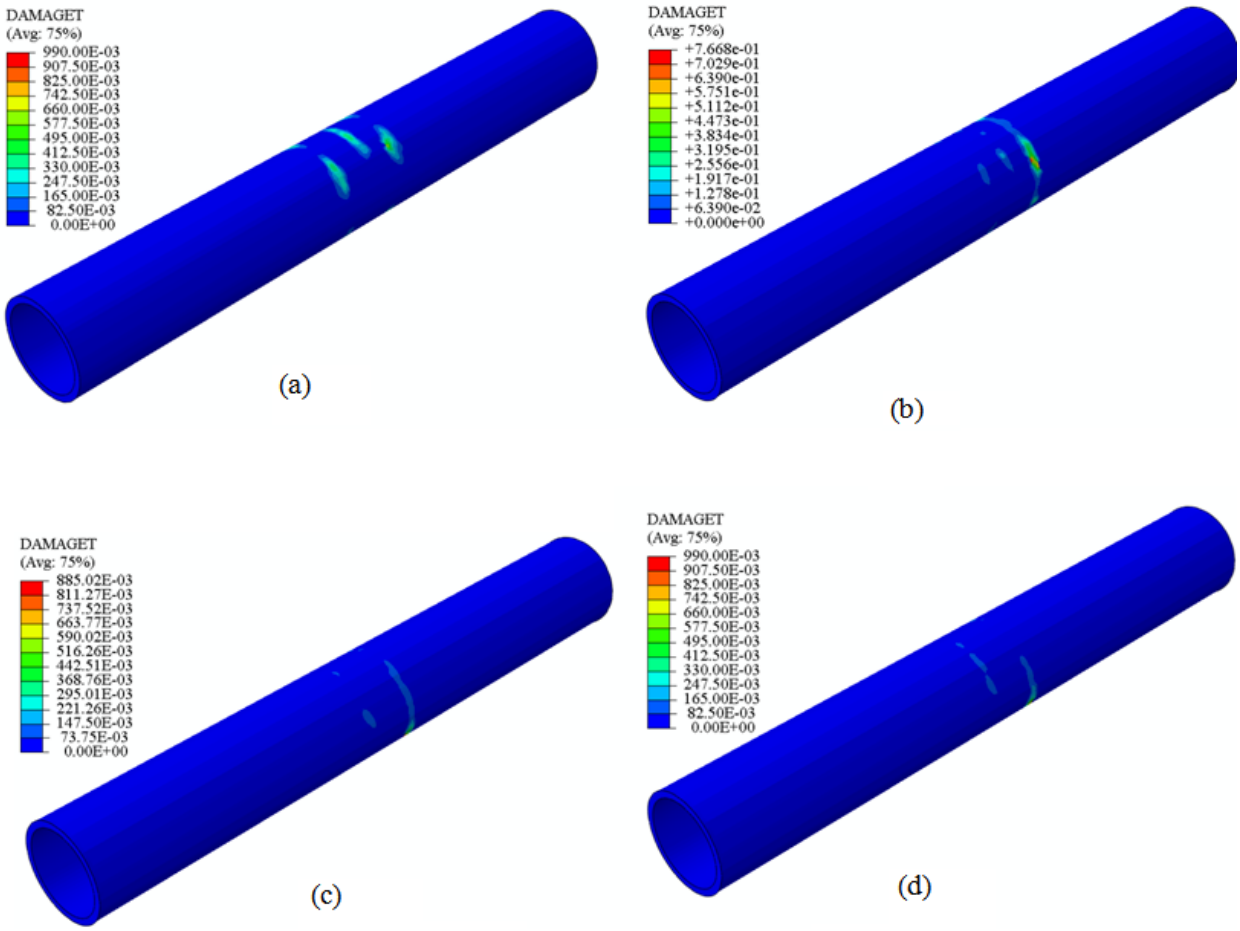

Figure 16. Tension damage contours in case of (a) 5m, (b) 15m, (c) 25m and (d) 35m of overburden depth

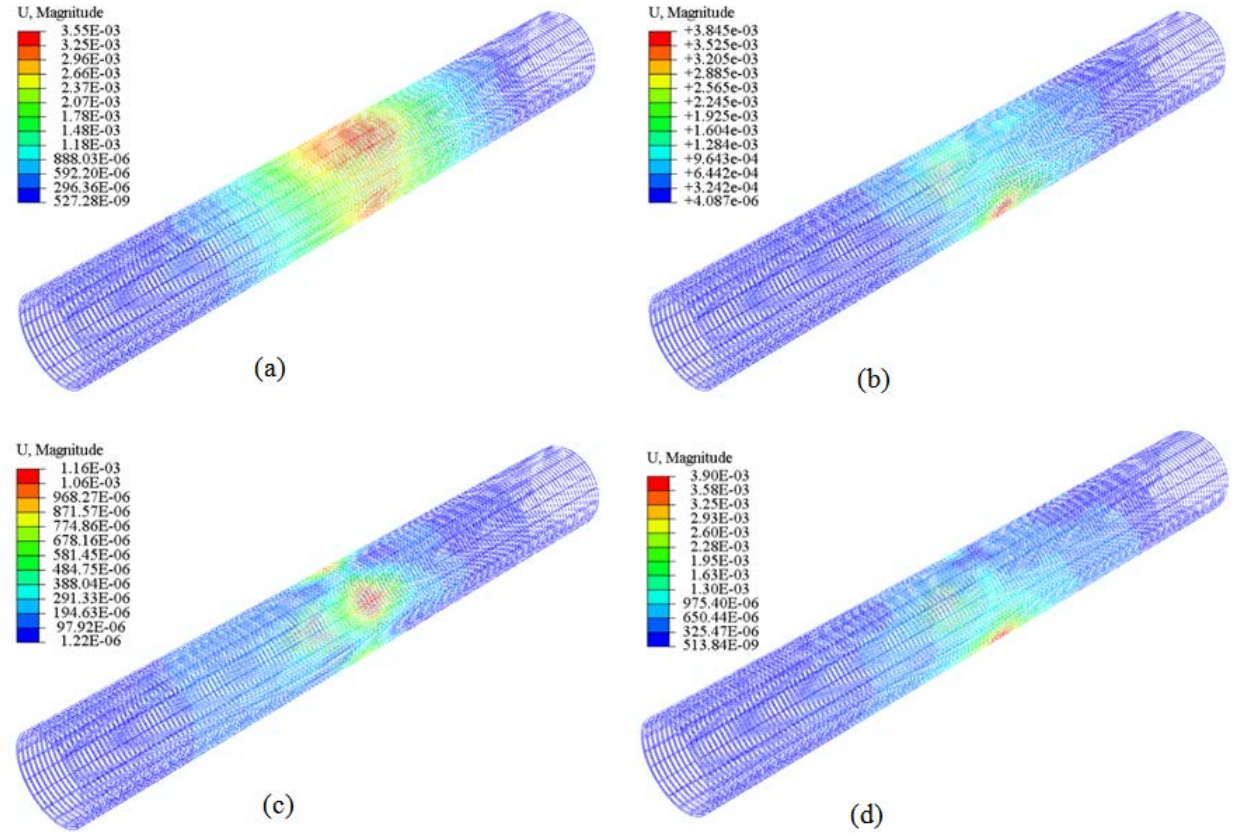

Figure 17. Displacement contours in of reinforcement cage case of (a) 5m, (b) 15m, (c) 25m and (d) 35m of overburden depth

Figure 16 has been plotted to compare the failure of concrete liner in cases of 5m, 15m, 25m and 35m of overburden depth in terms of tension damage caused by 100kg of TNT explosive. The tension damage has negligible i.e., less than one percent tensile failure and the concrete has a null failure in terms of compression, therefore, the contours of compression failure have not been shown here. It has been observed that as the overburden depth increases, there is a decrease in the magnitude of tension damage. Therefore, it may be concluded that as the overburden depth increases, and the tunnel has uniform in-situ stresses at the higher depth that makes the tunnel more stable against blast loading. Moreover, Figure 17 has been plotted to compare the displacement that occurred at the reinforcement cage embedded in the concrete liner of the tunnel. It has been observed that the only middle-central portion of the finite element model has experienced significant displacement in all the cases, except 5m overburden depth, which has more than half of tunnel length under blast effect. The magnitude of displacement in cases of 5m, 15m, 25m and 35m of overburden depth is 4.85mm, 3.55mm, 2.85mm and 1.40mm respectively. It has been concluded that displacement in the steel reinforcement is inversely proportional to the magnitude of overburden depth.

5. Conclusions

The present elastoplastic nonlinear continuum finite element simulation has incorporated the effect of weathering in terms of stratification, where highly weathered shale rock occurs at shallow depth. The Coupled-eulerian-lagrangian (CEL) method has been developed to simulate the internal blast-loading event due to 100 kg of TNT explosive. The finite element analysis has been carried out using Abaqus/Explicit and air has also been simulated in the present study. The results are extracted and compared to the different locations in the tunnel, i.e., ground, crown and invert in terms of displacement profile, displacement, velocity and acceleration variation with time. In addition, the tension damage contours have been compared for the different positions of the tunnel, i.e., 5m, 15m, 25m and 35m of overburden depth.

It has been concluded that the displacement magnitude at the ground, crown and invert locations are inversely proportional to the overburden depth because the lithostatic stresses increase with the increase in overburden depth making the tunnel more stable and resistant to different loading conditions. Also, it has been concluded that the displacement remains concentrated at the center of the tunnel in case of ground and crown positions, while a significantly larger portion of the tunnel has been subjected to blast loading damage. The deformation profile does not follow a traditional uniform profile; however, a V-shaped graph has been obtained in all the cases, except invert. The tension damage failure has been observed in all the cases, which was reduced with an increase in the overburden depth, however, the magnitude of tension damage is negligible. Also, the displacement in the steel reinforcement cage is concentrated at the center in a small portion of tunnel length, but more than half portion of the tunnel has been subjected to damage in case of 5m overburden depth due to blast loading.

Therefore, the tunnels should be simulated for extreme loading events especially blast loading if they are in a densely populated region of the world to strengthen them against any form of accidental or intentional attacks. Generally, researchers had considered a single rock block to simulate blast loading events, which does not comply with the actual field conditions. Therefore, layered stratified rocks must be taken into account for better results and understanding.

References

[1] Kenneth, S., Lane, (2019), "Tunnels and underground excavations | History, Methods, Uses, & Facts" | Britannica. https://www.britannica.com/technology/tunnel. Accessed 24 May 2020.

[2] Daphné Richemond-Barak (2017), "Underground Warfare", *Oxford University Press.*

[3] Ozacar, V., (2018), "New methodology to prevent blasting damages for the shallow tunnel", *Geomechanics and Engineering* 15(1227), 1227-1236.

[4] Chen, L., Zhou, Z., Zang, C., Zeng, L., Zhao, Y. (2019), "Failure pattern of large-scale goaf collapse and a controlled roof caving method used in gypsum mine", *Geomechanics and Engineering* 18: 449-457.

[5] Uyar, G.G., Aksoy, C.O., (2019), "Comparative review and interpretation of the conventional and new methods in blast vibration analyses", *Geomechanics and Engineering* 18(545).

[6] Kim, D.K. (2019), "Study on the characteristics of grout material using ground granulated blast furnace slag and carbon fiber", *Geomechanics and Engineering* 19(361), 361-368.

[7] Zaid, M., Sadique, M.R., (2020b), "Numerical modeling of internal blast loading on a rock tunnel", *Advances in Computational Design*, 5(4), , 417-443.

[8] Zaid, M., Shah, I.A., (2021a), "blast-resistant Stability Analysis of Triple Tunnel", *Advances in Geotechnics and Structural Engineering*, Springer, Singapore, pp 35-42.

[9] Zaid, M., Rehan, Sadique. M.R., (2021b), "A Simple Approximate Simulation Using Coupled Eulerian-Lagrangian (CEL) Simulation in Investigating Effects of Internal Blast in Rock Tunnel", *Indian Geotechnical Journal.* 1-18.

[10] Sadique, M.R., Zaid, M., Alam, M.M., (2021b), "Rock Tunnel Performance Under Blast Loading Through Finite Element Analysis" *Geotechnical and Geological Engineering*, 1-22.

[11] Dowding, C.H., Rozen, A.(1978), "Damage to rock tunnels for earthquake shaking", *Journal of Geotechnical Engineering Division* 104(175), 175-191.

[12] Gui, M.W., Chien, M.C., (2006), "Blast-resistant analysis for a tunnel passing beneath Taipei Shongsan airport - A parametric study". *Geotechnical and Geological Engineering*, 24(227), 227-248.

[13] Jain, S., Tiwari, R., Chakraborty, T., Matsagar, V., (2015), "Dynamic response of reinforced concrete wall under blast loading", *The Indian Concrete Journal*, 89(27), 27-41.

[14] Lu, Y., Xu, K. (2004), "Modelling of the dynamic behavior of concrete materials under blast loading". *International Journal of Solids and Structures*, 41(131), 131-143.

[15] Ragueneau, F., Gatuingt, F., (2003), "Inelastic behavior modeling of concrete in low and high strain rate dynamics", *Computers and Structures*, 81(1287), 1287-1299.

[16] Khan, S., Chakraborty, T., Matsagar, V. (2016), "Parametric Sensitivity Analysis and Uncertainty Quantification for Cast Iron-Lined Tunnels Embedded in Soil and Rock under Internal Blast Loading", *Journal of Performance of Constructed Facilities* 30.

[17] Wu, C., Lu, Y., Hao, H., (2004), "Numerical prediction of blast-induced stress wave from the large-scale underground explosion", *International Journal for Numerical and Analytical Methods in Geomechanics* 28(93), 93-109.

[18] Gahoi, A., Zaid, M., Mishra, S., Rao, K.S. (2017), "Numerical Analysis of the Tunnels Subjected to Impact Loading*", 7th Indian Rock Conference, Indorock2017*, New Delhi.

[19] Naqvi, M.W., Zaid, M., Sadique, M.R., Alam, M.M., (2017), "Dynamic Analysis of Rock Tunnels Considering Joint Dip Angle : A Finite Element Approach", *13th International Conference on Vibration Problems*, Indian Institute of Technology Guwahati, INDIA.

[20] Ali Khan, M., Sadique M. R., Zaid, M. (2019), "Effect of Stratification on Underground Opening: A Numerical Approach", *Advances in Transportation Engineering, Lecture Notes in Civil Engineering*,

[21] Athar, M. F., Zaid, M., Sadique, M.R. (2019), "Stability of Different shapes of Tunnels in Weathering Stages of Basalt", In *Proceedings of National Conference on Advances in Structural Technology*. NIT Silchar, 320-327.

[22] Zaid, M., Shah, I.A., Farooqi, M.A., (2019b), "Effect of Cover Depth in Unlined Himalayan Tunnel: A Finite Element Approach", *8th Indian Rock Conference*, New Delhi, pp 448-454.

[23] Zaid, M., Shah, I.A., (2021b), "Numerical Analysis of Himalayan Rock Tunnels under Static and Blast Loading", *Geotechnical and Geological Engineering*, 1-21.

[24] Zaid, M., Rehan, Sadique, M.R., (2021a), "Dynamic Analysis of Tunnels in Western Ghats of Indian Peninsula: Effect of Shape and Weathering", *Recent Trends in Civil Engineering. Springer, Singapore*, pp 763-776.

[25] Sadique, M.R., Zaid, M., Naqvi, M.W., Akhtar, M.F., (2021) "Analysis of Underground Renewable Energy Storage Tunnels Subjected to Capricious Superstructures", *Lecture Notes in Electrical Engineering 723* LNEE: 99-110.

[26] Sadique, M.R., Ali, A., Zaid, M., Alam, M.M., (2021a), "Experimental and Numerical Modeling of Tunneling-Induced Ground Settlement in Clayey Soil", *Lecture Notes in Civil Engineering 143* LNCE: 23-33..

[27] Zaid, M., Shah, I.A., Farooqi, M.A., (2019b), "Effect of Cover Depth in Unlined Himalayan Tunnel: A Finite Element Approach", 8th Indian Rock Conference, New Delhi, pp 448-454.

[28] Zaid, M., Mishra, S., (2021), "Numerical Analysis of Shallow Tunnels Under Static Loading: A Finite Element Approach" *Geotechnical and Geological Engineering* 39(), 1-27.

[29] Khan, M.A., Sadique, M.R., Harahap, I.H.,(2021), "Static and Dynamic Analysis of the Shielded Tunnel in Alluvium Soil with 2D FEM Model", *Transportation Infrastructure Geotechnology* 2021(1), 1-28.

[30] Bertuzzi R (2014), "Sydney sandstone and shale parameters for tunnel design", *Australian Geomechanics Journal*, 49(1), 1-10.

[31] Hafezolghorani, M., Hejazi, F., Vaghei, R.,(2015), "Simplified Damage Plasticity Model for Concrete" *Structural Engineering International*, IS456(2000) (2000) Plain and Reinforced Concrete - Code of Practice. Parliament of India, New Delhi.

[32] Zaid, M., Sadique, M.R., (2020c), "Blast resistant behavior of tunnels in sedimentary rocks", *International Journal of Protective Structures*, 204141962095121.

[33] Zaid, M., Sadique, M.R., (2020a), "The response of rock tunnel when subjected to blast loading: Finite element analysis. Engineering Reports".

[34] Zaid M, Sadique MR, Alam MM (2021e) Blast Resistant Analysis of Rock Tunnel Using Abaqus: Effect of Weathering. Geotechnical and Geological Engineering 2021 1-24.

[35] Zaid, M., Sadique, M.R., Alam, M.M., (2021d), "Blast analysis of tunnels in Manhattan-Schist and Quartz-Schist using coupled-Eulerian–Lagrangian method", *Innovative Infrastructure Solution*s, 6(69).

[36] Zaid, M., (2021b), "Dynamic stability analysis of rock tunnels subjected to impact loading with varying UCS", *Geomechanics and Engineering* 24(6), 505.

[37] Zhao, CF., Chen, J.Y., (2013), "Damage mechanism and mode of square reinforced concrete slab subjected to blast loading" *Theoretical and Applied Fracture Mechanics.* 63-64: 54-62.